362: Indoor climate control effect of AAC panels as determined by house model measurements and simulations

Yuko Tsukiyama [1]*, Nobuyuki Sunaga [2], Yosuke Chiba[1]

Asahi Kasei Homes Corporation R&D Laboratories,
*2-1 Samejima, Fuji-city, Shizuoka, 416-8501, Japan[1]**
tsukiyama.yb@om.asahi-kasei.co.jp
Dept. of Architecture and Building engineering, Tokyo Metropolitan Univ.,
1-1 Minami-osawa, Hachioji, Tokyo 192-0397, Japan[2]

Abstract

House model measurements and simulations were performed to determine the effects of autoclaved aerated concrete (AAC) heat capacity on interior temperature trends, for their application to development of low-energy thermally comfortable houses. Experimental measurement of natural and air-conditioned room air temperatures in the full-size simple house model comprised of AAC panels during 4-6 day periods in summer and winter showed the peak natural room air temperature to be about two hours behind the peak outside air temperature, as an effect of thermal storage by the AAC panels. The simulation technique was verified by comparison between the experimental measurement results and those of simple-model simulations for a house model similar to the experimental house model. Simulations of simple and general house models of AAC panel, RC, and wooden construction and varying heat capacities clearly showed that increasing the effective heat capacity reduced the indoor temperature variation but increased the energy load under intermittent a/c, and that 200-mm AAC panels with outside insulation in combination with cross ventilation and removable shading can substantially reduce a/c energy load and moderate temperature variation.

Keywords: houses with AAC panels, effectiveness of heat capacity, indoor thermal environment

1. Introduction

Passive design is an important technique for application of the natural energy of the environment to the achievement of comfort and energy conservation in housing. Much research has been reported on passive design with reinforced concrete (RC) and wooden housing, but very little on that with autoclaved aerated concrete (AAC), an inorganic architectural material composed of silica, quicklime, and cement and having an insulating effect due to its internal air cells. AAC panels are generally used in thicknesses of 50~100 mm in Japan. Their thermal conductivity is 0.17 W/mK and their volumetric heat capacity is 600 kJ/m^{3}K, both of which are similar to those of plywood, and their overall heat capacity as a building component may thus be expected to have a large effect on indoor thermal climate control.

We therefore investigated this effect by direct measurement and simulation, using simple and general house models of AAC panel, RC, and wood construction with various heat capacities.

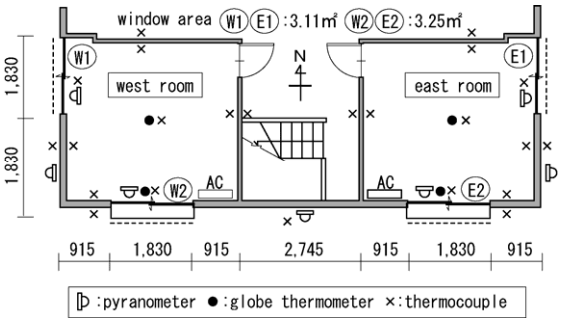

Fig 1. Floor plan and measurement points.

Fig 2. West room interior and outside views.

2. House model measurements

2.1 Overview

Measurements were first performed to determine the basic indoor climate of houses with AAC panels, using two actual-size simple house models consisting of the east and west rooms separated by a stairwell and atrium space as shown in Fig. 1 and 2, in a three-story house constructed with AAC panels in Itabashi-ku, Tokyo. The third floor was chosen to avoid sunlight blockage by nearby buildings. The two rooms were symmetrical, with openings in either the south and west or the east and south walls.

Each had a floor space of 13.4 m^2, and included floor and ceiling chambers. Insulation consisted of high-performance phenolic foam of 25 mm thickness in the exterior walls and rock wool of 100 mm thickness in the ceiling chamber. The AAC panels were installed outside the insulation materials of the walls and ceiling (details shown in Fig. 7). All measurements were performed in January-February and July-August 2005 using T-type thermocouples, globe thermometers, and pyranometers placed about 1 m above the floor level at the locations shown in Fig. 1, in summer modes without (Mode 1) and with (Mode 2) continuous air conditioning ("a/c") and winter modes without (Mode 3) and with (Mode 4) continuous a/c. The window configurations, air-conditioning settings, and time periods were all as shown in Table 1.Except for the east and west room, all rooms were not air-conditioned.

Table 1. Experimental modes.

mode		Room	Window in South	Window in East or West	AC	Day
1	Summer No Air-condition	East	Double-glazed Low-e glass	Double-glazed Low-e glass	×	2005/7/23 ~28
		West	Double-glazed Low-e glass	Double-glazed Low-e glass		
2	Summer with air-condition	East	Double-glazed Low-e glass	Double-glazed Low-e glass	27℃ all day	2005/8/15 ~19
		West	Double-glazed Low-e glass (reducing heat from the sun)	Double-glazed Low-e glass		
3	Winter No Air-condition	East	Double-glazed Low-e glass	Double-glazed Low-e glass	×	2005/1/12 ~17
		West	Double-glazed Low-e glass (reducing heat from the sun)	Double-glazed Low-e glass		
4	Winter with Air-condition	East	Double-glazed Low-e glass	Closed by the insulation	20℃ all day	2005/2/10 ~16
		West	Double-glazed Low-e glass (reducing heat from the sun)			

2.2 Summer measurements

The results of the Mode 1 and Mode 2 measurements are shown in Fig. 3 and 4. Note that in Mode 2 the glass in the south window of the west room was replaced by glass with solar radiation heat blocking glazing.

In Mode 1 (no a/c), the temperature in the east room with its east- and south-facing windows showed a peak about 5˚C lower than that of the west room with its west- and south-facing windows, but rose rapidly in the mid-morning hours and remained fairly stable at a high level thereafter. In both rooms, the temperatures were generally higher on the second day than on the first, presumably as an effect of heat accumulation.

In Mode 2 (with a/c), the air temperature in both rooms was stable at the a/c setting of 27˚C throughout the measurements, but the temperature pattern of the ceiling chamber air (approx. 100 mm height, between AAC panel and rock wool) was quite similar to that in Mode 1, with its daily peak around 17:00 or about 3 hr behind the outdoor temperature peak which occurred around 14:00, presumably as an effect of the heat capacity of the ceiling-chamber AAC panels.

2.3 Winter measurements

The results in Mode 3 (no a/c) and Mode 4 (with a/c) are shown in Fig. 5 and 6. In both modes, glass with solar radiation heat blocking glazing was used in the south window of the west room, and in Mode 4 the east and west windows were completely covered inside with insulation.

In Mode 3, the east room temperature rose to a peak of over 20˚C, but the heat accumulated in the daylight hours was insufficient to prevent a decline to less than 5˚C by early morning.

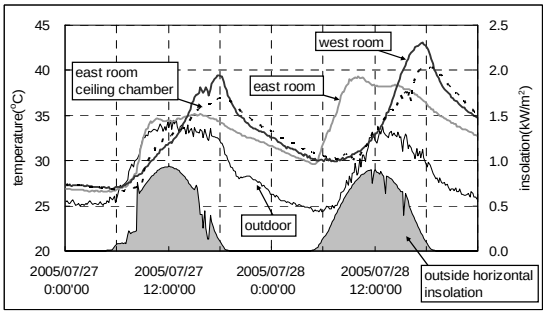

Fig 3. Temperature and insolation patterns in Mode 1.

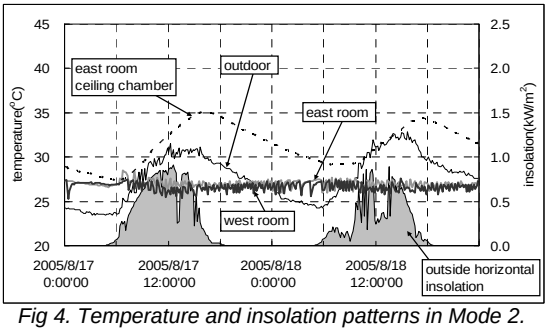

Fig 4. Temperature and insolation patterns in Mode 2.

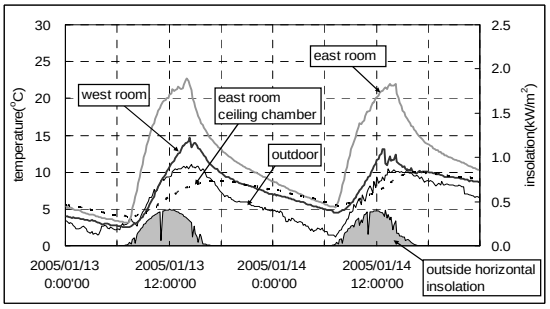

Fig 5. Temperature and insolation patterns in Mode 3.

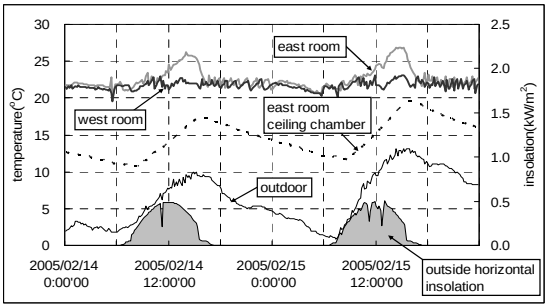

Fig 6. Temperature and insolation patterns in Mode 4.

In Mode 4, the heating effect of the sunlight in the east room raised the room temperature from 11:00 to 16:00 well above the a/c setting of 20˚C and the room temperature of about 22˚C at all other times, and the air temperature in the east room ceiling chamber was more than 5˚C higher than that in Mode 3 throughout the night and day.

3. Simple-model simulation

3.1 Overview

To investigate whether the interior thermal environment as obtained in the above experimental simple-model measurements was specific to its structure, we next performed simulations of the thermal environments in simple house models of AAC and wood construction,

using the TRNSYS [1] multizone dynamic thermal simulation program. The specifics of the simple-model components used in the simulation are described in Fig. 7. The model was a room of dimensions W3.66 x D3.66 x H2.4 m with ceiling and floor chambers, and thus similar to the experimental model. The weather data used in the simulation were taken from the Expanded AMeDAS Weather Data [2] for the standard year at Nerima, near the site of the experimental model.

3.2 Summer simulations

The results of the simulation for the summer AAC models, comprising one room having windows in the east and south walls (the "east room") and one with windows in the south and west walls (the "west room"), are shown in Fig. 8. Comparison of this figure with Mode 1 of Fig. 3 shows that, although the effect of solar heating via windows on the indoor temperature was somewhat greater in the simulation than in the experimental model, its indoor temperature pattern was quite similar to that of the experimental model. The simulation thus tended to confirm the characteristics of the internal thermal environment as found with the experimental model, though at a somewhat higher temperature level. For the following analyses, the east room was chosen as most representative.

Fig. 9 shows the results of the east room summer simulation for both the wooden and the AAC models. The daily range of room temperature variation is noticeably smaller in the AAC model variation. The delay in temperature peaks in the ceiling chambers from those of the outdoor temperature peaks is of particular note. In contrast to the wooden model, which showed no significant delay, the AAC model showed a 3 hr delay, which is clearly attributable to greater heat accumulation in the AAC roof panels.

3.3 Winter simulations

Fig. 10 shows the results of winter simulations using the east room with both windows closed and no a/c as the simple models for both AAC panel and wood houses. As in the summer simulations, the AAC model showed a milder daily variation in room temperatures, with a daily range of variation of only 16˚C as opposed to that of 20˚C in the wood model and thus again demonstrating the effect of the heat accumulation by the AAC. It should be noted, however, that the heating effect of the sunlight entering through the windows was not sufficient to obtain a comfortable thermal environment in either model.

4. General-model simulation

4.1 Overview

General-model simulations were performed, for full-scale AAC, RC and wooden house models, to further investigate and confirm the influence of the building components on indoor climate. The general-model simulations utilized the floor plan of Fig. 11 based on the House Standard Model of

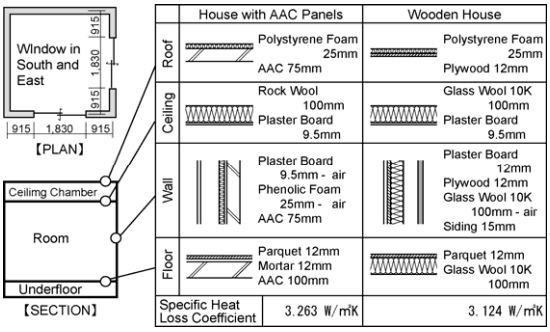

Fig 7. Specifics of simple-model components

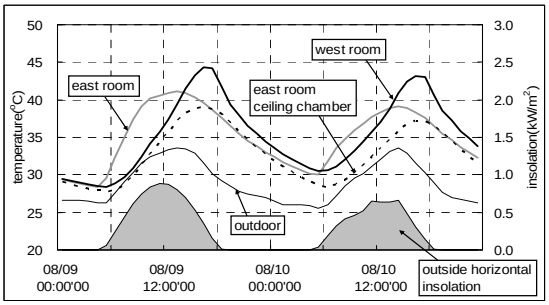

Fig 8. AAC no air conditioning fluctuation of temperature.

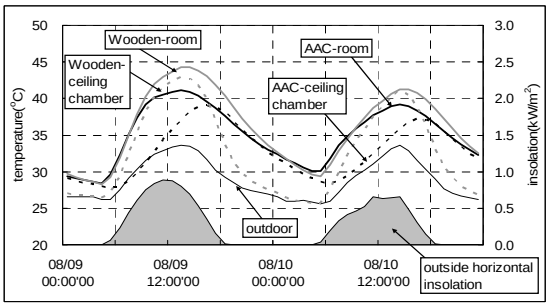

Fig 9. AAC and wood simple-model simulation, east room in summer with no a/c

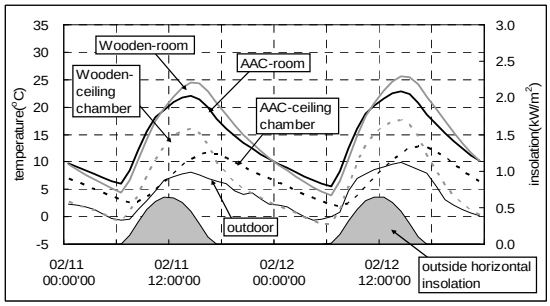

Fig 10. AAC and wood simple-model simulation, east room in winter with no a/c

the Architectural Institute of Japan [3] with variation in component compositions, a/c schedules, and other factors. The room temperature patterns and a/c loads were calculated. The specifics of the general-model components and their performance values are shown in Table 2.

In each model, all insulation thicknesses were chosen to match the standard performance values of the Next-generation Low-energy Standard in Japan Region IV (the "R-IV"), the thermal conductivity of the windows and doors was equivalent to 4.65 W/m^{2}K, and partition walls were composed of two layers of plasterboard each 12.5 mm thick.

The simulation program used in this study was composed of the COMIS [4] multizone ventilation

volume simulation program linked to the TRNSYS multizone dynamic thermal simulation program. The indoor heat generation and vaporization quantities were taken from the Residential Standard Schedule [5] of The Society of Heating Air-Conditioning and Sanitary Engineers of Japan, but those of the kitchen and bath rooms were excluded because of their large effects on room temperature. The weather data were taken from the AMeDAS standard year (1990~2000) data for Fuchu, Tokyo, which in heating degree-days is similar to the average values of R-IV. The simulation conditions in terms of the structural types are summarized in Table 2.

4.2 Effective heat capacity

The effective heat capacity of each structure was obtained by analytical solution of the range of wall internal temperature change [6] and compared with the a/c load, with the results as shown in Table 3. The winter and summer a/c settings were 20˚C and 27˚C, respectively. Only LD, MB, CR1, CR2 were air-conditioned. As shown, the effective heat capacity differed with the structure, with only small mutual differences in heating/cooling load under continuous and intermittent a/c, but the heating load under intermittent a/c varied substantially, in proportion to the effective heat capacity. In both effective heat capacity and heating/cooling load under intermittent a/c, the values found in the model AAC with outside insulation ("AAC-outside") were between those found in the models RC with outside insulation ("RC-outside") and RC with inside insulation ("RC-inside").

4.3 Winter temperature patterns

Fig. 12 and 13 show the living/dining-room (L/D) temperature patterns with no a/c and intermittent a/c, respectively, on the typical winter days of February 1~2.

With no a/c, the daily range of temperature variation found for RC-outside, with its large effective heat capacity, was 7.8˚C. This was considerably smaller than the ranges found for the other models. The temperature variation for AAC-outside was similar to that for RC-inside but between the AAC-outside and the RC-inside was delayed by about 1 hr in temperature rise and fall, as an affect of the AAC thermal capacity. There was little difference between the AAC-models in maximum and minimum temperatures, which suggests that the effect of the AAC heat accumulation on the indoor environment was of relatively short duration.

In the intermittent a/c mode, the a/c was turned on for 3 hr before noon, 2 hr in the early afternoon, and 6 hr in the evening, the times when persons would most likely be in the L/D. Following the morning a/c, solar heat served to warm the RC-outside structure but the indoor temperature did not rise, whereas in all of the other models the solar heat raised the indoor temperatures and the natural environment was sufficient to maintain an indoor temperature of 20˚C without a/c heating during the 2-hr afternoon a/c engagement period. It thus appears that an absence of a/c heating cessation in the RC-outside model may be the reason for the high a/c heating load found for that structure in winter with intermittent a/c.

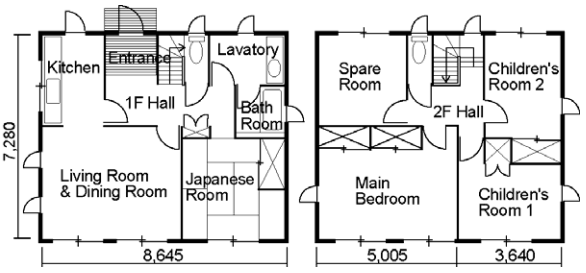

Fig 11. Floor plan of general house model

Table 2. General-model components and U-values

	ceiling	external wall	western floor	mezzanine floor
① wooden house	slate12 plywood12 air PF79 PB12	mortar30 plywood9 air PF31 PB12	parquet10 plywood12 PF33	carpet15 plywood12 air PB12
	K=0.240W/m²K	K=0.530W/m²K	K=0.480W/m²K	
Q=2.35W/m²K				
② AAC inside insulation	AAC100 PF60 air PB12	AAC75 air7 PF22 air PB12	parquet13 plywood12 PF21 AAC100	parquet13 mortar12 AAC100 air PB12
	K=0.240W/m²K	K=0.530W/m²K	K=0.480W/m²K	
Q=2.36W/m²K				
③ AAC outside insulation	PF60 AAC100 air PB12	PF22 air7 AAC75 air PB12	parquet13 plywood12 AAC100 PF21	
	K=0.240W/m²K	K=0.530W/m²K	K=0.480W/m²K	
Q=2.36W/m²K				
④ RC inside insulation	RC130 PF80 air PB12	aluminium siding 2 air RC150 PF30 PB12	vinyltile5 PF33 mortar35 RC130	parquet10 plywood20 RC130 air PB12
	K=0.240W/m²K	K=0.530W/m²K	K=0.480W/m²K	
Q=2.35W/m²K				
⑤ RC outside insulation	PF80 RC130 air PB12	aluminium siding 2 air PF30 RC150 PB12	vinyltile5 mortar35 RC130 PF33	
	K=0.240W/m²K	K=0.530W/m²K	K=0.480W/m²K	
Q=2.35W/m²K				

Table 3. Effective heat capacity and annual load

	Effective heat capacity(MJ/K)	Intermittent a/c (MJ/m²Y) Winter	Summer	Annual	Continuous a/c (MJ/m²Y) Winter	Summer	Annual
①Wooden	5.3	107.1	65.6	172.7	262.2	104.6	366.9
②AAC-in.	8.2	120.1	63.4	183.5	264.3	97.7	362.0
③AAC-out.	13.7	129.8	65.2	195.0	263.6	98.4	362.0
④RC-in.	11.1	125.4	63.2	188.6	269.3	98.4	367.7
⑤RC-out.	37.3	148.9	63.4	212.3	265.0	92.9	357.8

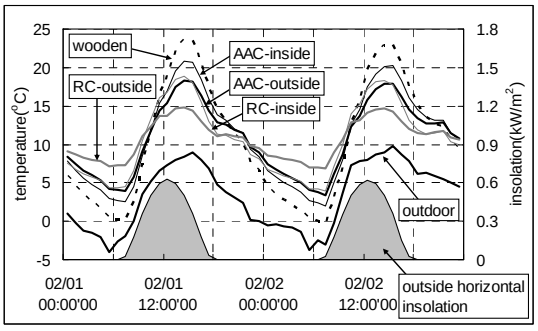

Fig 12. Winter temperature patterns in L/D with no a/c.

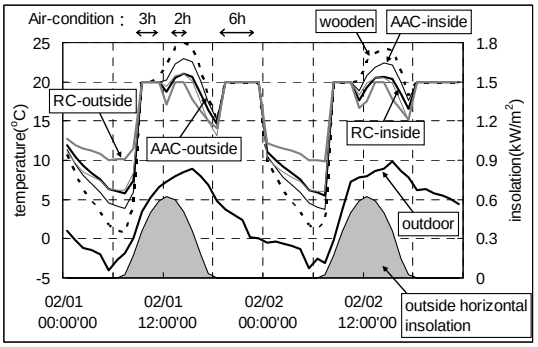

Fig 13. Winter temperature patterns in L/D with intermittent a/c.

At night, following the 6-hr a/c engagement, all of the models showed falling temperatures. In the wooden model, the temperature had fallen to a very low minimum by dawn, thus suggesting that although this structure may exhibit a low heating load it may also involve an environment of low comfort prior to a/c engagement in the morning. The AAC-outside temperature pattern during the same hours was similar to that of RC-inside, and in conjunction with the daytime patterns indicated that the AAC-outside structure provides a relatively moderate pattern of temperature change throughout the day and during the night following sunset.

All of the winter simulations, taken together, show a tendency by AAC for shorter periods of heat accumulation and release than those of RC.

4.4 Summer temperature patterns

Fig. 14 and 15 show the L/D room temperature patterns with cross ventilation by two open windows and with intermittent a/c, respectively, on the typical summer days of September 4~5.

In the cross-ventilation mode, the south and west windows in the living room were open whenever the outside temperature was 26˚C or more, and thus from 8:00 to 18:00 on both of these days. No other windows in the model were open at any time.

As the house model included no sunlight blocking or shading devices, the room temperature during cross ventilation remained higher than the outside temperature as an effect of solar heating.

The high effective heat capacity of RC in the RC-outside model moderated the temperature rise during cross ventilation in daytime, but the room temperature remained high following closure of the windows and throughout the night due to radiation of the heat it had accumulated in the daylight hours.

The RC-outside showed a similar tendency in the intermittent a/c mode. In the daylight hours, the rise in room temperature after each a/c period was comparatively small, but the temperature stayed comparatively high throughout the night after the evening a/c disengagement.

Throughout the summer, as in the winter, the temperature pattern of the AAC-outside model generally resembled that of the RC-inside model, but was distinguished by a more moderate temperature rise following the morning period of 3-hr a/c, in accordance with a faster rate of heat radiation by AAC.

4.5 Annual temperature patterns

Fig. 16 shows the annual temperature pattern for each of the general-house models with and without a/c, as the monthly minimum, average, and maximum indoor temperature of that model, with the indoor temperature calculated as the average of the temperatures in all of its rooms at any given time.

With or without a/c, little or no difference was found among the models in their monthly average temperatures despite their differing structures. In terms of monthly minimum and maximum temperature, the RC-outside model showed a

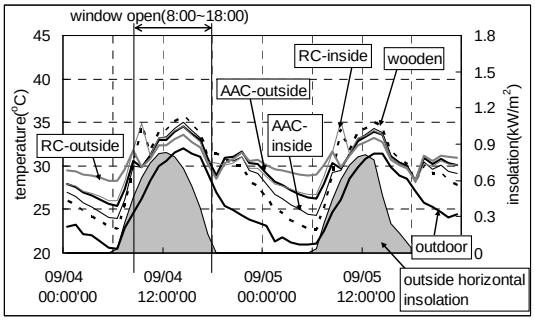

Fig 14. Summer temperature patterns in L/D with cross ventilation

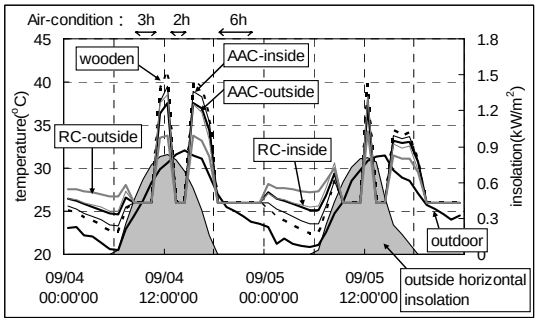

Fig 15. Summer temperature patterns in L/D with intermittent a/c

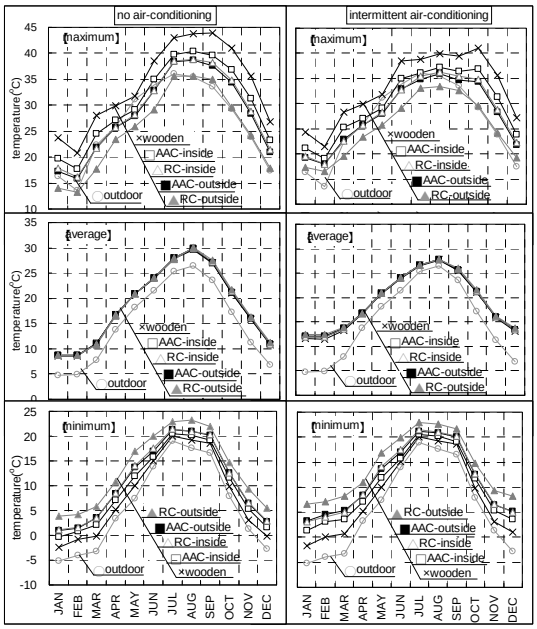

Fig 16. Annual temperature patterns,, with and without intermittent a/c.

smaller range of variation during the year than the others in both modes, as an effect of its higher effective heat capacity. In contrast the wood model, with the lowest of all effective heat capacities, showed the highest range of variation in both modes.

With no a/c, the annual pattern of the AAC-outside model approached that of the RC-inside model. With intermittent a/c, AAC-inside model approached that of the RC-inside model.

It may be noted that the low minimum indoor temperatures observed for all the general-house winter simulations apparently resulted from a degree of insulation that was insufficient in accumulated heat retention, and particularly the adoption of the low U-value openings.

4.6. Design parameters and energy load

Simulation in the L/D was performed to investigate the effects of AAC panel thickness, cross ventilation, and overhang shading. The a/c schedule of all models was intermittent, and in the cross-ventilation mode the windows were open whenever the L/D temperature was 22˚C or more and the outside temperature was between 24˚C and 30˚C. The AAC-outside configuration was used throughout.

Table 4 shows the maximum, minimum, and average outdoor and indoor temperatures in the months of February and August, and the high minimum indoor temperatures of February obtained with AAC panels of 200 mm thickness and the low maximum indoor temperatures in August obtained with cross ventilation and/or shading in combination with the 100-mm panels.

Fig. 17 shows the annual heating and cooling loads for the L/D.

With no cross ventilation or shading, the 200-mm panels enabled the greatest reduction in total energy consumption. As compared with the 100-mm panel levels, the reduction enabled by the 200-mm panels was about the same as that enabled by the 300-mm panels for cooling load but the heating load of 300-mm panels is much greater than that of 200-mm panels. Cross ventilation reduced the cooling load by more than one-half but did not moderate the maximum indoor temperature in August. The use of shading in combination with the cross ventilation reduced both the cooling load and the maximum indoor temperature, but increased the heating load.

The results indicate that 200-mm panels in combination with cross ventilation and removable shading can effectively reduce energy load and temperature variation.

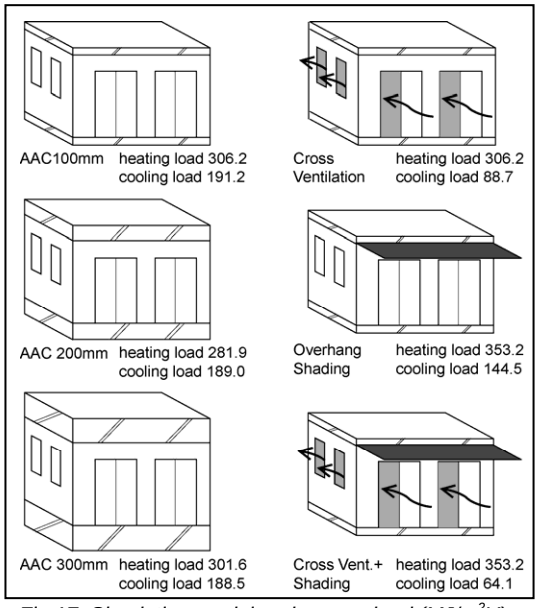

Fig 17. Simulation model and energy load (MJ/m²Y)

Table 4. Outdoor and indoor temperatures (˚C).

		Outdoor	AAC 100mm	AAC 200mm	AAC 300mm	Cross Ventilation	Ovehang Shading	Cross Vent. +Shad.
Feb.	max	13.6	22.9	23.1	22.7	22.9	20.0	20.0
	min	-4.0	5.0	6.2	5.7	5.0	5.0	5.0
	ave	4.9	15.9	16.2	16.0	15.9	15.4	15.4
Aug.	max	35.5	39.1	38.6	38.5	39.4	35.4	35.5
	min	17.6	21.3	21.9	21.8	21.3	21.2	21.2
	ave	26.5	27.5	27.6	27.6	28.3	27.0	27.7

5. Conclusion

This basic investigation on the indoor thermal effects of AAC panels, by full-size simple-model measurements and simple- and general-model simulations of AAC, RC, and wood houses, revealed the following.

(1) Experimental measurements showed ceiling-chamber temperatures substantially lagging behind outside temperature trends, and confirmed thus confirming an influence on indoor temperatures by AAC roof, wall, and floor panels.

(2) Simple-model simulation showed the range of daily indoor temperature variation to be substantially smaller in the AAC model than in the wood model, thus demonstrating the effect of AAC heat accumulation on room temperature.

(3) Effective heat capacity affected the heating load under intermittent a/c, but had little effect on cooling load under intermittent a/c or heating/cooling load under continuous a/c.

(4) General-model simulation showed the indoor temperature with AAC to lag behind that with RC by about 1 hr, and indicated the effects of AAC heat accumulation to be of shorter duration.

(5) Under intermittent a/c, increasing the effective heat capacity reduced the indoor temperature variation and increased the a/c energy load, and decreasing the effective heat capacity had the reverse effect.

(6) The effect of AAC-inside on annual temperature variation was similar to that of RC-inside with no a/c, and that of AAC-outside was similar to that of RC-inside under intermittent a/c.

(7) Simulation in the L/D indicated that 200-mm AAC panels in combination with cross ventilation and removable shading can substantially reduce a/c energy load and moderate temperature variation.

The results, in summary, showed AAC-outside to be intermediate to the other structures in its effects, both without a/c and with a/c.

Further investigations are contemplated to elucidate the relation between AAC effective heat capacity and indoor thermal environment through full-scale experiments and simulations.

6. References

1. TRNSYS 16 (2007), A Transient System Simulation Program, User Manuals: Solar Energy Laboratory, University of Wisconsin-Madison.

2. Expanded AMeDAS Weather Data (2005), Architectural Institute of Japan.

3. M. Udagawa (1985), A Proposal of Standard Problem: Heat Symposium 15, p23-33.

4. COMIS 3.2 (2005), Conjunction of Multizone Infiltration Specialists, EMPA.

5. Schedule ver.2.0 (2000), Life Schedule Generation Program: The Society of Heating Air-Conditioning and Sanitary Engineers of Japan.

6. N. Sunaga (1992), Study on The Effect of Thermal Mass on Indoor Climate Control with Solar Energy: p.171-174.